Persymmetric Adaptive Target Detection With Distributed MIMO Radar

JUN LIU, Member, IEEE
Xidian University, China

HONGBIN LI, Senior Member, IEEE
Stevens Institute of Technology
Hoboken, NJ, USA

BRAHAM HIMED, Fellow, IEEE
Air Force Research Laboratory
Wright Patterson Air Force Base, OH, USA

Based on persymmetric structures in received signals, we consider the adaptive detection problem in colored Gaussian noise with unknown persymmetric covariance matrix in a multiple-input, multiple-output (MIMO) radar with spatially dispersed antennas. To this end, a set of secondary data for each transmit-receive pair is assumed to be available. A MIMO version of the persymmetric generalized likelihood ratio test (MIMO-PGLRT) detector is proposed. A closed-form expression for the probability of false alarm of this detector is derived. In addition, a MIMO version of the persymmetric sample matrix inversion (MIMO-PSMI) detector is also developed. Compared to the MIMO-PGLRT detector, MIMO-PSMI has a simpler form and is computationally more efficient. Numerical examples are provided to demonstrate that the proposed two detection algorithms can significantly alleviate the requirement of the amount of secondary data and allow for a noticeable improvement in detection performance.

Manuscript received October 7, 2013; revised June 16, 2014; released for publication June 18, 2014.

DOI. No. 10.1109/TAES.2014.130652.

Refereeing of this contribution was handled by L. Kaplan.

This work was supported in part by a subcontract with Dynetics, Inc. for research sponsored by the Air Force Research Laboratory (AFRL) under Contract FA8650-08-D-1303.

Authors' addresses: J. Liu was with Stevens Institute of Technology. He is now with the National Laboratory of Radar Signal Processing, Xidian University, Xi'an, 710071, China; H. Li, Stevens Institute of Technology, Department of Electrical and Computer Engineering, Castle Point on Hudson, Hoboken, NJ 07030. E-mail: (hli@stevens.edu); B. Himed, RF Technology Branch, Air Force Research Laboratory, 2241 Avionics Circle, Bldg 620, WPAFB, OH 45433.

I. INTRODUCTION

The paradigm of multiple-input, multiple-output (MIMO), which originated in communications, is more and more widely applied to radars [1–5]. In general, MIMO radar falls into two classes according to the configuration of its antennas, one with colocated antennas [6–8] and the other with widely distributed antennas [9–14]. We restrict ourselves to the second MIMO radar configuration, which for brevity is referred to as MIMO radar in the following.

In [15], several temporal coherent adaptive detectors are proposed to deal with the problem of target detection in MIMO radar. A set of training data is employed for each transmit-receive pair to estimate the unknown clutter covariance matrix. The performance analysis in [15] is conducted by resorting to Monte Carlo simulations because of the lack of theoretical expressions for the probabilities of false alarm and detection. In [16], a MIMO version of the generalized likelihood ratio test (MIMO-GLRT) detector, which is an extension of the detector in [15, Eq. (19)], is developed, and its false alarm rate is obtained in closed form. The problem of moving target detection with distributed MIMO radar is also considered in [17] where a MIMO version of the adaptive matched filter (MIMO-AMF) detector is proposed. It is shown that the number of training data has a great impact on the detection performance of the MIMO radar [15, 17]. Particularly, the detection performance is significantly degraded when the number of training data is small. In many practical scenarios, it is difficult to collect a large number of independent identically distributed target-free training data due to many factors such as variations in terrain [18] and interfering targets [19, 20]. Therefore, it is interesting to investigate how to achieve satisfactory detection performance when the amount of training data is limited.

Some prior knowledge about the structure of clutter covariance matrix (e.g., persymmetric structure) may be exploited to alleviate the requirement of the amount of training data [21–25]. In practical applications, the clutter covariance matrix has a Hermitian persymmetric (also called centrohermitian) form, when a detection system is equipped with a symmetrically spaced linear array [26, chap. 7] or symmetrically spaced pulse trains [27]. Hermitian persymmetry has a property of doubly symmetry, i.e., Hermitian about its principal diagonal and persymmetric about its cross diagonal. Unless otherwise stated, "persymmetric" always denotes "Hermitian persymmetric" for brevity in the following.

The investigation on the persymmetric structure of clutter covariance matrix can be traced to Nitzberg's paper [28], where the maximum likelihood (ML) estimate of the persymmetric covariance matrix was obtained. Using this ML estimate, Cai and Wang developed two persymmetric detection algorithms, i.e., the persymmetric multiband GLRT algorithm [27] and the persymmetric sample matrix inversion (SMI) algorithm [29]. In recent years, several

other detection algorithms have been proposed with a-priori information on the persymmetric structure of the clutter covariance (see [30–36]). All these persymmetric detection algorithms mentioned above validate the fact that an obvious gain in detection performance can be obtained by exploiting persymmetric structures in the clutter covariance, especially when the amount of training data available is limited.

In this study, we examine the adaptive detection problem in the presence of colored Gaussian noise with unknown covariance matrix in a distributed MIMO radar by using persymmetric structures in the received data. The unknown noise covariance matrix for each transmit-receive pair is estimated from a set of secondary data. A MIMO version of the persymmetric GLRT detector, referred to as the MIMO-PGLRT detector, is proposed, whose false alarm rate is derived in closed form. Moreover, we develop a MIMO version of the persymmetric SMI detector, referred to as the MIMO-PSMI detector, which is simpler than the former detector, and thus has lower computational complexity. Interestingly, both persymmetric detection algorithms bear a constant false alarm rate (CFAR) property with respect to the noise covariance matrix. Simulation results reveal that compared to the conventional MIMO-GLRT and MIMO-AMF detectors that do not use the persymmetric structure, both of the proposed detectors obtain significant gains in detection performance, especially when the amount of secondary data is limited. Additionally, the MIMO-PGLRT detector outperforms the MIMO-PSMI detector, even though a higher computational burden is incurred. However, the performance difference among these four MIMO detectors is negligible when the amount of training data is adequate.

1) *Notation*: Vectors (matrices) are denoted by boldface lower (upper) case letters. Superscripts $(\cdot)^T$, $(\cdot)^*$, and $(\cdot)^\dagger$ denote transpose, complex conjugate, and complex conjugate transpose, respectively. The notation $\sim$ means "is distributed as," and $\mathcal{CN}$ denotes a circularly symmetric, complex Gaussian distribution. $\mathbf{I}_p$ stands for a p-dimensional identity matrix. $|\cdot|$ represents the modulus of a complex number and $\jmath = \sqrt{-1}$. The determinant and trace of a matrix are denoted by $\det(\cdot)$ and $\mathrm{tr}(\cdot)$, respectively. $\Re\mathrm{e}(\cdot)$ and $\Im\mathrm{m}(\cdot)$ represent the real and imaginary parts of a complex quantity, respectively.

II. SIGNAL MODEL

In this section, a signal model for MIMO radar with widely distributed antennas is presented. Suppose that a MIMO radar consists of M transmit antennas and N receive antennas that are geographically dispersed. The total number of transmit-receive paths available is $V = MN$. Assume that the tth transmitter sends Q_t pulses, and a target to be detected does not leave the cell under test during these pulses. We further impose the standard assumption that all transmit waveforms are orthogonal to each other, and each receiver uses a bank of M matched filters corresponding to the M orthogonal waveforms.

Sampled at the pulse rate via slow-time sampling, the signal received by the rth receive antenna due to the transmission from the tth transmit antenna, which is usually called test data (primary data), can be expressed as a $Q_t \times 1$ vector, i.e.,

$$\mathbf{x}_{r,t} = a_{r,t}\,\mathbf{s}_{r,t} + \mathbf{n}_{r,t}, \tag{1}$$

where $\mathbf{s}_{r,t} \in \mathbb{C}^{Q_t \times 1}$ denotes a known $Q_t \times 1$ steering vector for the target relative to the tth transmitter and rth receiver pair [12, 17]; $a_{r,t} \in \mathbb{C}$ is a deterministic but unknown complex scalar accounting for the target reflectivity and the channel propagation effects in the tth transmitter and rth receiver pair; the noise $\mathbf{n}_{r,t} \sim \mathcal{CN}(\mathbf{0}, \mathbf{R}_{r,t})$, where $\mathbf{R}_{r,t}$ is a positive definite covariance matrix of dimension $Q_t \times Q_t$.

These primary data vector $\{\mathbf{x}_{r,t}\}$ can be assumed to be independent of each other due to the widely distributed antennas in the MIMO radar. Notice that in the above model (1), these steering vectors $\mathbf{s}_{r,t}$s are not necessarily identical even though they describe the same target, since the relative position and velocity of the target with respect to different widely dispersed radars may be distinct. In addition, the covariance matrices $\mathbf{R}_{r,t}$s are also not constrained to be the same, because the statistical properties of the noise may be unique for each transmit-receive perspective. We further assume that $Q_t > 1$, $t = 1, 2, \ldots, M$, such that coherent processing for each test data is possible. Note that Q_t, $t = 1, 2, \ldots, M$ are not constrained to be identical, which means that the numbers of the pulses transmitted by different transmit antennas may be distinct. Another standard assumption we impose is that for each test data vector $\mathbf{x}_{r,t}$, there exists a set of training data (secondary data) free of target signal components, i.e., $\{\mathbf{y}_{r,t}(k), k = 1, 2, \ldots, K_{r,t} | \mathbf{y}_{r,t}(k) \sim \mathcal{CN}(\mathbf{0}, \mathbf{R}_{r,t})\}$. Here, we require $K_{r,t} \geq Q_t/2$ to guarantee a nonsingular covariance matrix estimate with unit probability [27]. Note that the numbers of secondary data vectors $K_{r,t}$ are not constrained to be the same. Suppose further that these secondary data vectors are independent of each other and of the primary data vectors.

The detection problem considered herein involve structured $\mathbf{R}_{r,t}$ and $\mathbf{s}_{r,t}$. Specifically, it is supposed that each of the $\mathbf{R}_{r,t}$s has the persymmetric property, i.e., $\mathbf{R}_{r,t} = \mathbf{J}\mathbf{R}_{r,t}^*\mathbf{J}$ where $\mathbf{J}$ is a permutation matrix with unit antidiagonal elements and zeros elsewhere, namely,

$$\begin{bmatrix} 0 & 0 & \cdots & 0 & 1 \\ 0 & 0 & \cdots & 1 & 0 \\ \vdots & \vdots & \vdots & \vdots & \vdots \\ 0 & 1 & \cdots & 0 & 0 \\ 1 & 0 & \cdots & 0 & 0 \end{bmatrix}. \tag{2}$$

In addition, the steering vector is also assumed to be a persymmetric one satisfying $\mathbf{s}_{r,t} = \mathbf{J}\mathbf{s}_{r,t}^*$. The above assumption on the structures of $\mathbf{R}_{r,t}$ and $\mathbf{s}_{r,t}$ is valid when each antenna in the MIMO radar uses a pulse train

symmetrically spaced with respect to its midtime delay for temporal domain processing. In the common case of pulse trains with uniform spacing, the steering vector $\mathbf{s}_{r,t}$ has the form:

$$\mathbf{s}_{r,t} = \left[\mathrm{e}^{-J\frac{(Q_t-1)2\pi\bar{f}_{r,t}}{2}}, \ldots, \mathrm{e}^{-J\,2\pi\bar{f}_{r,t}}, 1, \mathrm{e}^{J\,2\pi\bar{f}_{r,t}}, \ldots, \mathrm{e}^{J\frac{(Q_t-1)2\pi\bar{f}_{r,t}}{2}}\right]^T, \tag{3}$$

where $\bar{f}_{r,t}$ defined similarly as [12, Eq. (2)] is the normalized target Doppler shift corresponding to the tth transmitter and rth receiver pair.

Let the null hypothesis (H_0) be such that the primary data is free of the target signal and the alternative hypothesis (H_1) be such that the primary data contains the target signal. Hence, the detection problem is to decide between the null hypothesis and the alternative one:

$$H_0 : \begin{cases} \mathbf{x}_{r,t} \sim \mathcal{CN}(\mathbf{0}, \mathbf{R}_{r,t}) \\ \mathbf{y}_{r,t}(k) \sim \mathcal{CN}(\mathbf{0}, \mathbf{R}_{r,t}) \end{cases} \tag{4a}$$

and

$$H_1 : \begin{cases} \mathbf{x}_{r,t} \sim \mathcal{CN}(a_{r,t}\,\mathbf{s}_{r,t}, \mathbf{R}_{r,t}) \\ \mathbf{y}_{r,t}(k) \sim \mathcal{CN}(\mathbf{0}, \mathbf{R}_{r,t}) \end{cases} \tag{4b}$$

for $t = 1, 2, \ldots, M$, $r = 1, 2, \ldots, N$, and $k = 1, 2, \ldots, K_{r,t}$. In [15–17], MIMO detection algorithms were developed without using any prior knowledge about the special structure of the noise covariance matrix. In the sequel, two adaptive detectors are proposed by exploiting the persymmetric structures of $\mathbf{R}_{r,t}$ and $\mathbf{s}_{r,t}$. It will be seen that the exploitation of persymmetry can bring in a noticeable detection gain.

III. MIMO-PGLRT DETECTOR

A. MIMO-PGLRT Detector

Because of the unknown parameters $a_{r,t}$ and $\mathbf{R}_{r,t}$, the Neyman-Pearson criterion cannot be employed. According to the GLRT, a practical detector can be obtained by replacing all the unknown parameters with their ML estimates, i.e., the detector is obtained by

$$\frac{\max_{\{a_{r,t},\,\mathbf{R}_{r,t}\,|\,t=1,2,\ldots,M,r=1,2,\ldots,N\}} f(\mathbf{X}|H_1)}{\max_{\{\mathbf{R}_{r,t}\,|\,t=1,2,\ldots,M,r=1,2,\ldots,N\}} f(\mathbf{X}|H_0)} \underset{H_0}{\overset{H_1}{\gtrless}} \lambda_0, \tag{5}$$

where λ_0 is the detection threshold, $f(\cdot)$ denotes probability density function (PDF), and $\mathbf{X} = \{\mathbf{X}_{1,1}, \ldots, \mathbf{X}_{N,M}\}$ with $\mathbf{X}_{r,t} = [\mathbf{x}_{r,t}, \mathbf{y}_{r,t}(1), \mathbf{y}_{r,t}(2), \ldots, \mathbf{y}_{r,t}(K_{r,t})]$. Due to the independent assumption on these test data vectors, the PDF of $\mathbf{X}$ under H_q ($q = 0, 1$) can be represented as

$$f(\mathbf{X}|H_q) = \prod_{r=1}^{N}\prod_{t=1}^{M} \underbrace{f_{\mathbf{X}_{r,t}}(\mathbf{X}_{r,t}|H_q)}_{\triangleq f_{r,t,q}}, \quad q = 0,1, \tag{6}$$

where

$$f_{r,t,q} = \left\{\frac{1}{\pi^{Q_t}\det(\mathbf{R}_{r,t})}\exp\left[-\mathrm{tr}(\mathbf{R}_{r,t}^{-1}\mathbf{T}_{r,t,q})\right]\right\}^{K_{r,t}+1} \tag{7}$$

with

$$\mathbf{T}_{r,t,q} = \frac{1}{K_{r,t}+1}\left[\sum_{k=1}^{K_{r,t}} \mathbf{y}_{r,t}(k)\mathbf{y}_{r,t}^{\dagger}(k) + (\mathbf{x}_{r,t} - q a_{r,t}\,\mathbf{s}_{r,t})(\mathbf{x}_{r,t} - q a_{r,t}\,\mathbf{s}_{r,t})^{\dagger}\right]. \tag{8}$$

Define

$$\hat{\mathbf{R}}_{r,t} = \frac{1}{2}\sum_{k=1}^{K_{r,t}} \left\{\mathbf{y}_{r,t}(k)\mathbf{y}_{r,t}^{\dagger}(k) + \mathbf{J}[\mathbf{y}_{r,t}(k)\mathbf{y}_{r,t}^{\dagger}(k)]^*\mathbf{J}\right\} \tag{9}$$

$$\mathbf{x}_{r,t}^{\mathrm{e}} = \frac{1}{2}\left[(\mathbf{I}+\mathbf{J})\Re\mathfrak{e}(\mathbf{x}_{r,t}) - (\mathbf{I}-\mathbf{J})\Im\mathfrak{m}(\mathbf{x}_{r,t})\right] \tag{10}$$

$$\mathbf{x}_{r,t}^{\mathrm{o}} = \frac{1}{2}\left[(\mathbf{I}-\mathbf{J})\Re\mathfrak{e}(\mathbf{x}_{r,t}) + (\mathbf{I}+\mathbf{J})\Im\mathfrak{m}(\mathbf{x}_{r,t})\right] \tag{11}$$

and

$$\tilde{\mathbf{X}}_{r,t} = [\mathbf{x}_{r,t}^{\mathrm{e}}, \mathbf{x}_{r,t}^{\mathrm{o}}]. \tag{12}$$

As derived in Appendix A, the detector is given by

$$\prod_{r=1}^{N}\prod_{t=1}^{M}\left(\frac{1}{1-\Phi_{r,t}}\right)^{K_{r,t}+1} \underset{H_0}{\overset{H_1}{\gtrless}} \lambda_0, \tag{13}$$

where

$$\Phi_{r,t} = \frac{\tilde{\mathbf{s}}_{r,t}^{\dagger}\tilde{\mathbf{R}}_{r,t}^{-1}\tilde{\mathbf{X}}_{r,t}(\mathbf{I}_2 + \tilde{\mathbf{X}}_{r,t}^{\dagger}\tilde{\mathbf{R}}_{r,t}^{-1}\tilde{\mathbf{X}}_{r,t})^{-1}\tilde{\mathbf{X}}_{r,t}^{\dagger}\tilde{\mathbf{R}}_{r,t}^{-1}\tilde{\mathbf{s}}_{r,t}}{\tilde{\mathbf{s}}_{r,t}^{\dagger}\tilde{\mathbf{R}}_{r,t}^{-1}\tilde{\mathbf{s}}_{r,t}} \tag{14}$$

with

$$\tilde{\mathbf{s}}_{r,t} = \Re\mathfrak{e}(\mathbf{s}_{r,t}) - \Im\mathfrak{m}(\mathbf{s}_{r,t}), \tag{15}$$

and

$$\tilde{\mathbf{R}}_{r,t} = \Re\mathfrak{e}(\hat{\mathbf{R}}_{r,t}) + \mathbf{J}\Im\mathfrak{m}(\hat{\mathbf{R}}_{r,t}). \tag{16}$$

Here, (13) is referred to as the MIMO-PGLRT detector.

Note that there exists a significant difference between the detector (13) developed in [27] and the MIMO-PGLRT detector (13) derived here. In [27], the noise covariance matrices at multiple bands are assumed to be identical, whereas in our study, the noise covariance matrices at different transmit-receive pairs may be distinct.

B. Performance Analysis

In order to complete the construction of the test in (13), we should provide an approach to set the detection threshold. In this section, we derive a closed-form expression for the probability of false alarm of the MIMO-PGLRT detector, which can be employed to compute the detection threshold for any given probability of false alarm. In doing so, we take the logarithm of (13), namely,

$$\Lambda = \sum_{r=1}^{N}\sum_{t=1}^{M}(K_{r,t}+1)\ln\left(\frac{1}{1-\Phi_{r,t}}\right) \underset{H_0}{\overset{H_1}{\gtrless}} \lambda, \tag{17}$$

where $\lambda = \ln\lambda_0$.

Define

$$\alpha_{r,t} = \frac{2K_{r,t} + 2}{2K_{r,t} - Q_t + 1}. \tag{18}$$

We relabel $\alpha_{1,1}, \ldots, \alpha_{1,M}, \ldots, \alpha_{N,1}, \ldots, \alpha_{N,M}$ as $\alpha_1, \alpha_2, \ldots, \alpha_V$, respectively, where $V = MN$. As shown in Appendix B, (17) has a statistically equivalent form as follows:

$$\Lambda = \sum_{i=1}^{V} \alpha_i \Omega_i \underset{H_0}{\overset{H_1}{\gtrless}} \lambda, \tag{19}$$

where the PDF of Ω_i under hypothesis H_0 is the standard exponential distribution as seen in (56), and the random variables Ω_i are independent of one another. It is worth noting that the test statistic Λ under H_0 is exactly a sum of weighted exponential variables Ω_i.

Recall that some Q_ts may be identical, and so are some $K_{r,t}$s. Thus, some α_is may be equal. We denote these coefficients with the same value by a new symbol, i.e., α_1, $\alpha_2, \ldots, \alpha_V$ are denoted by $e_1, e_2, \ldots, e_s$ ($e_n \neq e_m$ for $n \neq m$), where s is the total number of the coefficients with different values, and e_i corresponds to some coefficient whose value is repeated $d_i + 1$ times among $\alpha_1, \alpha_2, \ldots, \alpha_V$. In addition, $d_i \geq 0$, $i = 1, 2, \ldots, s$ and $s + \sum_{i=1}^{s} d_i = V$.

According to Theorem 3 of [37], the probability of false alarm of the MIMO-PGLRT detector can be expressed as

$$P_{\mathrm{FA}} = \left(\prod_{i=1}^{s} d_i ! \right)^{-1} \frac{\partial^{d_1+d_2+\ldots+d_s}}{\partial e_1^{d_1} \partial e_2^{d_2} \ldots \partial e_s^{d_s}} \left[\sum_{n=1}^{s} \frac{J_V(e_n, \lambda)}{E_n} \right], \tag{20}$$

where the operator $\frac{\partial^{d_1+d_2+\ldots+d_s}}{\partial e_1^{d_1} \partial e_2^{d_2} \ldots \partial e_s^{d_s}}(\cdot)$ denotes the mixed $(d_1 + d_2 + \ldots + d_s)$th order partial derivatives of a function with respect to $e_1, e_2, \ldots, e_s$,

$$J_L(x, T) = x^L \exp(-Tx^{-1}) \tag{21}$$

and

$$E_n = e_n \prod_{j=1, j\neq n}^{s} (e_n - e_j). \tag{22}$$

Note that for $n = 1$, we have $E_1 = e_1$.

In particular, the expression (20) bears a simple form for the following two cases.

1) *Case I*: $\alpha_1, \alpha_2, \ldots, \alpha_V$ are all the same. At this moment, $s = 1$, $E_1 = e_1 = \alpha_1$ and $d_1 = V - 1$. Then, we have

$$\sum_{n=1}^{s} \frac{J_V(e_n, \lambda)}{E_n} = J_{V-1}(e_1, \lambda). \tag{23}$$

Thus, the probability of false alarm for this case is

$$\begin{aligned} P_{\mathrm{FA}} &= \frac{1}{(V-1)!} \frac{\partial^{V-1}}{\partial e_1^{V-1}} [J_{V-1}(e_1, \lambda)] \\ &= \frac{\exp(-\lambda e_1^{-1})}{(V-1)!} \sum_{n=0}^{V-1} \mathrm{C}_{V-1}^{n} (V - 1 - n)! \lambda^n e_1^{-n} \\ &= \exp(-\lambda e_1^{-1}) \sum_{n=0}^{V-1} \frac{1}{n!} (\lambda e_1^{-1})^n, \end{aligned} \tag{24}$$

where the second equality is obtained with the Lemma in [38], and $\mathrm{C}_m^n = \frac{m!}{n!(m-n)!}$.

2) *Case II*: $\alpha_1, \alpha_2, \ldots, \alpha_V$ are all distinct. In this case, $s = V$ and $d_k = 0$, $e_k = \alpha_k$ for $k = 1, 2, \ldots, V$. Therefore, the probability of false alarm for this case can be simplified as

$$P_{\mathrm{FA}} = \sum_{n=1}^{V} \frac{J_V(e_n, \lambda)}{E_n} = \sum_{n=1}^{V} \frac{e_n^V \exp(-\lambda e_n^{-1})}{E_n}. \tag{25}$$

For the general case where parts of α_i's are identical, we can use (20) to obtain the false alarm rate of the MIMO-PGLRT detector. As an example, we consider the case in which $V = 4$, $\alpha_2 = \alpha_3$, but α_1, α_2 and α_4 are all different. In this case, the expression for the probability of false alarm of the MIMO-PGLRT detector can be represented by

$$\begin{aligned} P_{\mathrm{FA}} &= \frac{1}{0!1!0!} \frac{\partial}{\partial e_2} \left[\sum_{j=1}^{3} \frac{J_4(e_j, \lambda)}{E_j} \right] \\ &= \frac{e_1^3 \exp(-\lambda e_1^{-1})}{(e_1 - e_2)^2 (e_1 - e_3)} + \frac{e_2(3e_2 + \lambda) \exp(-\lambda e_2^{-1})}{(e_2 - e_1)(e_2 - e_3)} \\ &\quad - \frac{e_2^3 (2e_2 - e_1 - e_3) \exp(-\lambda e_2^{-1})}{(e_2 - e_1)^2 (e_2 - e_3)^2} \\ &\quad + \frac{e_3^3 \exp(-\lambda e_3^{-1})}{(e_3 - e_1)(e_3 - e_2)^2}. \end{aligned} \tag{26}$$

It is obvious that the probability of false alarm of the MIMO-PGLRT detector does not depend on the noise covariance matrix. Therefore, the MIMO-PGLRT detector exhibits the desirable CFAR property against the noise covariance matrices.

It can be seen from the above derivation that the closed-form expression for the probability of false alarm of the MIMO-PGLRT detector is obtained with the fact that under H_0 the individual test statistic $\Phi_{r,t}$ in the MIMO-PGLRT detector has a simple right-tail probability as seen in (52), and thus has a simple PDF as seen in (54). However, the right-tail probability of $\Phi_{r,t}$ under H_1 contains a one-dimensional integral (see [27, Eq. (16)]). Therefore, the detection probability of the MIMO-PGLRT detector is analytically intractable.

IV. MIMO-PSMI DETECTOR

In this section, an alternative solution to the detection problem (4) is proposed, which has a lower computational burden than the MIMO-PGLRT detector. To this end, an approach similar to that in [29] is employed. More specifically, for each transmit-receive pair, we use the following test statistic:

$$\Xi_{r,t} = |\mathbf{w}_{r,t}^{\dagger} \mathbf{x}_{r,t}^{\mathrm{e}}|^2 + |\mathbf{w}_{r,t}^{\dagger} \mathbf{x}_{r,t}^{\mathrm{o}}|^2, \tag{27}$$

where $\mathbf{x}^{\mathrm{e}}_{r,t}$ and $\mathbf{x}^{\mathrm{o}}_{r,t}$ are defined in (10) and (11), respectively, and the weight vector $\mathbf{w}_{r,t}$ is given by

$$\mathbf{w}_{r,t} = \frac{\tilde{\mathbf{R}}^{-1}_{r,t}\tilde{\mathbf{s}}_{r,t}}{(\tilde{\mathbf{s}}^{\dagger}_{r,t}\tilde{\mathbf{R}}^{-1}_{r,t}\tilde{\mathbf{s}}_{r,t})^{1/2}}. \tag{28}$$

Jointly processing the independent data received by all the transmit-receive pairs, we have the following decision rule:

$$\Xi = \sum_{r=1}^{N}\sum_{t=1}^{M}\Xi_{r,t} = \sum_{r=1}^{N}\sum_{t=1}^{M}\frac{\tilde{\mathbf{s}}^{\dagger}_{r,t}\tilde{\mathbf{R}}^{-1}_{r,t}\tilde{\mathbf{X}}_{r,t}\tilde{\mathbf{X}}^{\dagger}_{r,t}\tilde{\mathbf{R}}^{-1}_{r,t}\tilde{\mathbf{s}}_{r,t}}{\tilde{\mathbf{s}}^{\dagger}_{r,t}\tilde{\mathbf{R}}^{-1}_{r,t}\tilde{\mathbf{s}}_{r,t}} \underset{H_0}{\overset{H_1}{\gtrless}} \xi, \tag{29}$$

where ξ is the detection threshold. Here, (29) is referred to as the MIMO-PSMI detector.

Note that Ξ in (29) is different from the test statistic in [29, Eq. (13)], since the weight vectors $\mathbf{w}_{r,t}$ in (28) are distinct for different transmit-receive pairs, whereas the weight vectors in [29, Eq. (13)] are all the same. Compared with the MIMO-PGLRT detector in (13), the MIMO-PSMI detector in (29) has a simpler structure. More specifically, (29) does not need to compute the term $(\mathbf{I}_2 + \tilde{\mathbf{X}}^{\dagger}_{r,t}\tilde{\mathbf{R}}^{-1}_{r,t}\tilde{\mathbf{X}}_{r,t})^{-1}$, and thus is computationally more efficient.

As to the theoretical performance of the MIMO-PSMI detector, unfortunately, closed-form expressions for the probabilities of false alarm and detection are both intractable, since the right-tail probability of its constituent test statistic $\Xi_{r,t}$ under H_0 or H_1 includes a one-dimensional integral (see [29, Eqs. (14) and (15)]). Nevertheless, we can observe from [29, Eq. (14)] that the statistical property of the test statistic $\Xi_{r,t}$ under H_0 is irrelevant to the noise covariance matrix. As expected, the MIMO-PSMI detector consisting of $\Xi_{r,t}$'s possesses the CFAR property with respect to all the noise covariance matrices.

V. SIMULATIONS RESULTS

In this section, numerical simulations are conducted to validate the above theoretical analysis and illustrate the performance of the proposed two detectors. For simplicity, we consider a MIMO radar made up of two transmit antennas and two receive antennas (i.e., $M = N = 2$), and each transmit antenna sends nine coherent pulses with equal spacing (i.e., $Q_1 = Q_2 = 9$). The steering vector $\mathbf{s}_{r,t}$ has the form as seen in (3). Suppose further that the normalized Doppler shifts of the target are 0.1, 0.2, 0.3, and 0.4 for the (1,1), (1,2), (2,1), and (2,2) transmit-receive pairs, respectively. The (i, j)th element of the noise covariance matrix is chosen to be $[\mathbf{R}]_{i,j} = \sigma^2\, 0.95^{|i-j|}$, where σ^2 represents the noise power. Note that the covariance matrices for all transmit-receive pairs are set to be identical for simplicity. Nevertheless, we estimate the covariance matrix for a specific transmit-receive pair by using only the training data collected in that corresponding transmit-receive pair, instead of using all training data from all transmit-receive pairs. Without loss of generality, $a_{r,t}$s are supposed to be the same, and then can be uniformly denoted by a. The signal-to-noise ratio (SNR) is defined by

$$\mathrm{SNR} = 10\log_{10}\frac{|a|^2}{\sigma^2}. \tag{30}$$

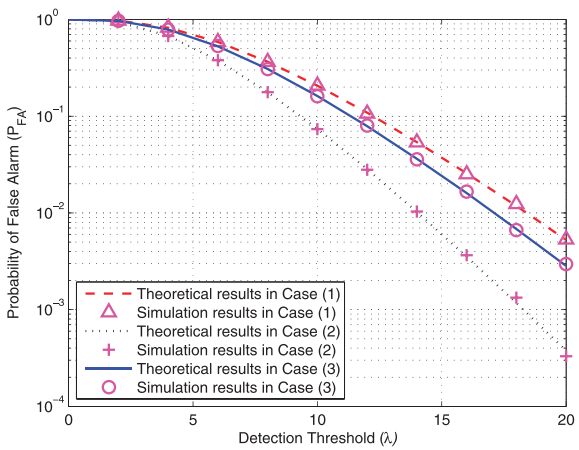

Fig. 1. Probability of false alarm of MIMO-PGLRT detector in three cases. Dashed, dotted, and solid lines indicate results obtained from (24), (25), and (26) for Cases (1), (2), and (3), respectively. Symbols Δ, o, and $+$ denote corresponding results obtained from Monte Carlo simulations.

We consider three cases with different number of secondary data, namely,

- Case (1): $K_{1,1} = K_{1,2} = K_{2,1} = K_{2,2} = 10$, i.e., α_i's defined in (18) are all identical;
- Case (2): $K_{1,1} = 14$, $K_{1,2} = 16$, $K_{2,1} = 18$ and $K_{2,2} = 20$, i.e., α_i's are all distinct;
- Case (3): $K_{1,1} = 12$, $K_{1,2} = K_{2,1} = 10$ and $K_{2,2} = 14$, i.e., $\alpha_2 = \alpha_3$, but α_1, α_2, α_4 are all distinct.

The probability of false alarm of the MIMO-PGLRT detector as a function of the detection threshold λ for the above three cases is shown in Fig. 1, where the dashed, dotted and solid lines denote the results obtained from (24), (25), and (26) for Cases (1), (2), and (3), respectively, and the symbols represent the corresponding results obtained from Monte Carlo simulations. The number of independent trials used in each case is 10^5. It is shown that the simulation results match the theoretical results pretty well.

The detection probability curves of the proposed persymmetric detectors versus SNR for the above three cases are plotted with Monte Carlo simulations in Fig. 2, where the probability of false alarm is set to be 10^{-3}. For comparison purpose, the MIMO-GLRT detector in [16] and the MIMO-AMF detector (19) in [17], both of which do not utilize a-priori knowledge about the persymmetric structure of the noise covariance matrix, are considered. Notice that the MIMO-AMF detector in [17, Eq. (19)] is derived based on the assumption that each transmit-receive pair uses the same number of secondary data. Therefore, the performance of the MIMO-AMF

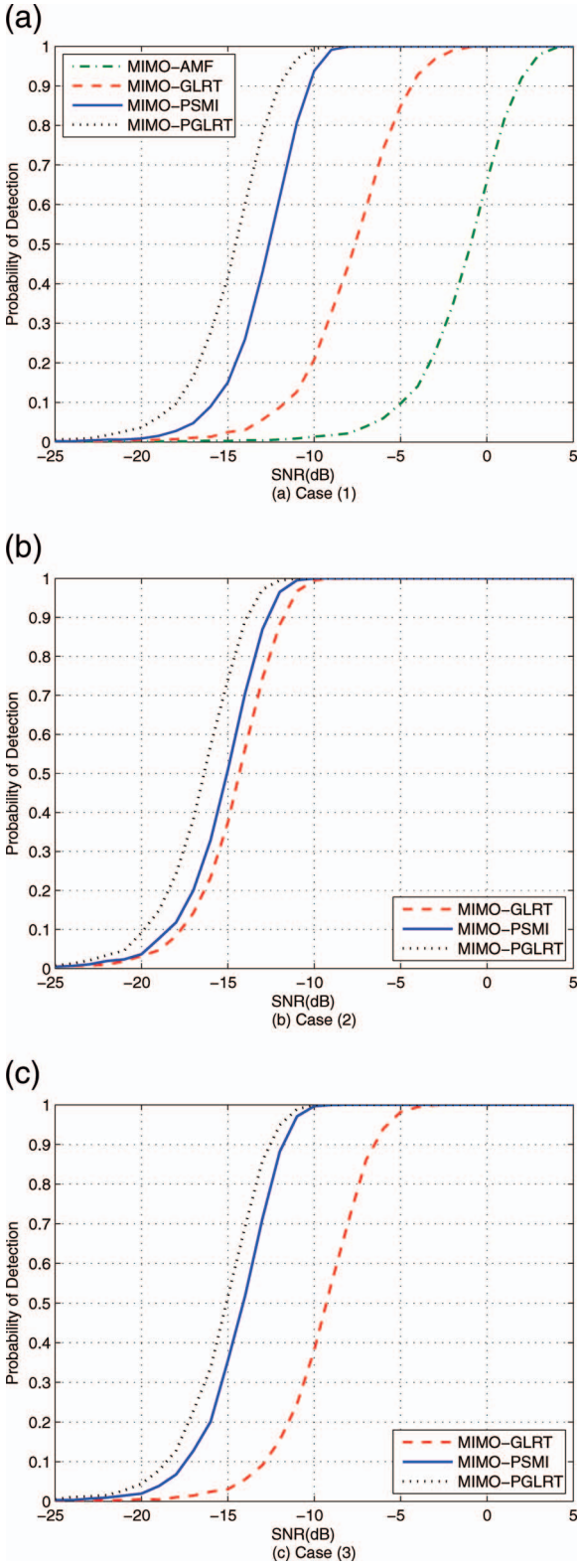

Fig. 2. Performance comparisons between three detectors with fixed $P_{\mathrm{FA}} = 10^{-3}$ in three cases. Dotted-dashed, dashed, solid, and dotted lines indicate detection probabilities obtained with Monte Carlo simulations for MIMO-AMF, MIMO-GLRT, MIMO-PSMI, and MIMO-PGLRT detectors, respectively.

detector is presented only in Case (1) (see Fig. 2a). The number of independent trials used to obtain each value of the detection probability is 5000.

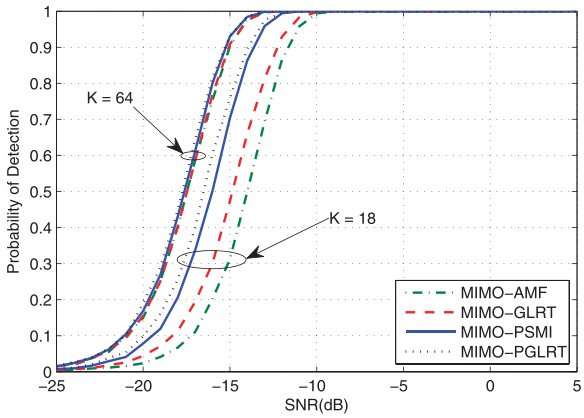

Fig. 3. Performance comparisons between three detectors with different amount of secondary data for fixed $P_{\mathrm{FA}} = 10^{-3}$. Each transmit-receive pair has same number of secondary data that is uniformly denoted by K. Dotted-dashed, dashed, solid, and dotted lines indicate detection probabilities obtained with Monte Carlo simulations for MIMO-AMF, MIMO-GLRT, MIMO-PSMI, and MIMO-PGLRT detectors, respectively.

Comparing the detection performance of the same detector in different cases, we can see that increasing the amount of secondary data improves the performance. This is because the use of more secondary date samples can improve the accuracy in estimating the noise covariance matrix, hence leading to a gain in detection performance.

It can also be observed in Fig. 2 that in each case taken into consideration, the MIMO-PGLRT detector performs the best, the MIMO-PSMI detector has slightly inferior performance, and the MIMO-GLRT or MIMO-AMF detector achieves the worst performance. In particular, the performance gains of the MIMO-PGLRT detector and the MIMO-PSMI detector with respect to the MIMO-AMF detector in Case (1) are about 14 and 12 dB, respectively, when the detection probability is 0.9. Obviously, the MIMO-PSMI and MIMO-PGLRT detectors outperform the MIMO-GLRT and MIMO-AMF detectors due to the exploitation of a priori knowledge about the persymmetric structures in the received signals. In addition, the MIMO-PSMI detector performs worse than the MIMO-PGLRT detector but with the benefit of lower computational burden.

Nevertheless, these four detectors considered here may perform almost similarly when the number of secondary data is sufficient. This can be seen in Fig. 3 (along with Fig. 2a) where performance comparisons among these detectors are presented with different numbers of secondary data. It is assumed that each transmit-receive pair has the same number of secondary data which is uniformly denoted by K. As shown in Fig. 3, the performance difference between these detectors can be negligible in the case of sufficient secondary data (for instance, $K = 64$ in this example). This is due to the fact that using sufficient secondary data, one can obtain a high accuracy in the noise covariance matrix estimate, even without a priori information on the persymmetric

structures. Hence, when sufficient secondary data are available, the MIMO-PSMI detector is highly recommended because of its relatively low computational burden and negligible performance loss.

The above simulations are conducted by assuming that there is no mismatch in the persymmetric structure of covariance matrix. In practice, the covariance matrix may deviate from the persymmetric structure due to spacing errors in coherent pulses or array processing. In what follows, we illuminate the effects of a mismatch in the persymmetric structure of covariance matrix on the performance of the considered detectors. We construct the noise covariance matrix as $\mathbf{R} = \frac{\sigma^2}{2}(\mathbf{R}_1 + \mathbf{R}_1^{\dagger})$, where each entry of $\mathbf{R}_1$ is independently sampled from a uniform distribution on the range [0, 1]. Note that the noise covariance matrix $\mathbf{R}$ is Hermitian but not necessarily persymmetric.

Fig. 4 presents the detection performance of four detectors for different training data sizes in the mismatch case. It can be seen that in this mismatch case, the MIMO-PGLRT (or MIMO-PSMI) detector provides a detection performance better than the MIMO-GLRT (or MIMO-AMF) detector when the number of training data is limited (for instance, $K = 10$ in this example). This observation in the mismatch case is the same as that in the match case (compare Fig. 2a and Fig. 4a). However, the MIMO-GLRT (or MIMO-AMF) detector outperforms the MIMO-PGLRT (or MIMO-PSMI) detector when the number of training data is large (for instance, $K = 36$ in this example). This phenomenon can be easily explained. In fact, the detection performance in the mismatch case is related to two factors: the persymmetric mismatch and the training data size. In the case of sufficient training data, the exploitation of the mismatched persymmetric structure does not necessarily lead to a performance gain.

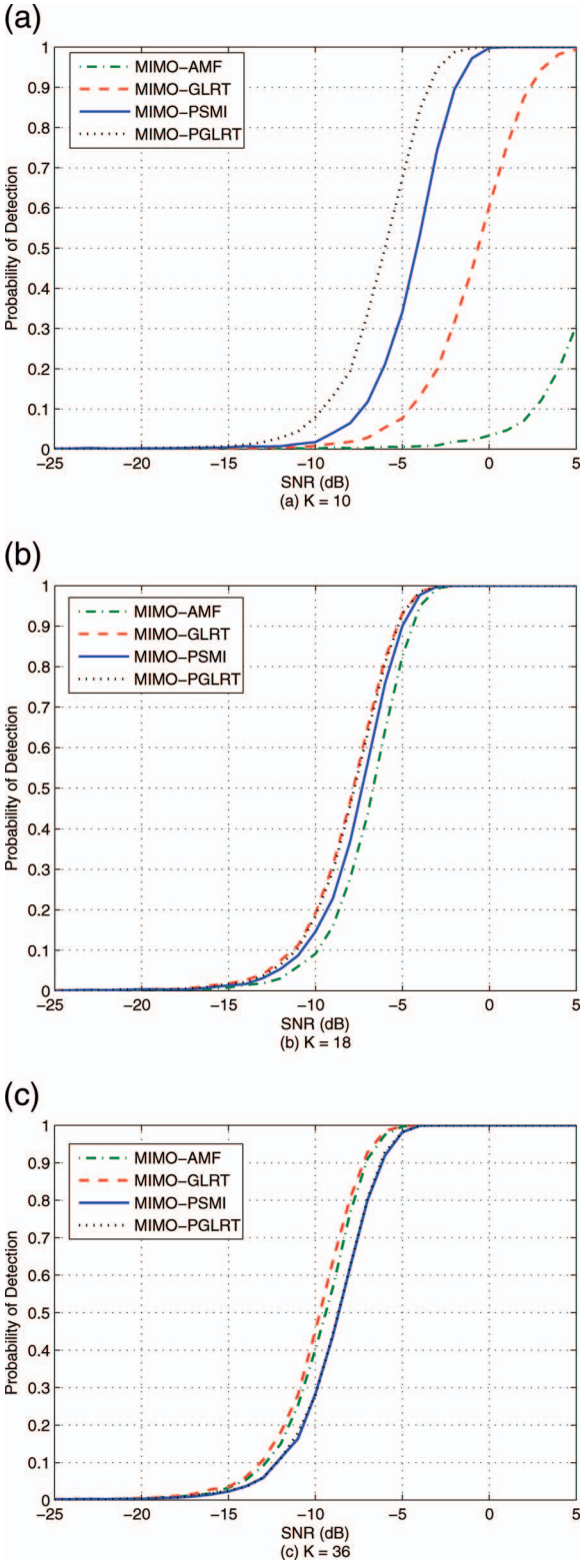

Fig. 4. Performance comparisons for fixed $P_{\mathrm{FA}} = 10^{-3}$ in mismatch case. Each transmit-receive pair has same number of secondary data that is uniformly denoted by K: (a) $K = 10$; (b) $K = 18$; (c) $K = 36$.

VI. CONCLUSION

In this paper, we propose two persymmetric detectors (i.e., MIMO-PGLRT and MIMO-PSMI) in a distributed MIMO radar by exploiting persymmetric structures in received signals. The probability of false alarm of the MIMO-PGLRT detector is obtained in closed form, which is validated with Monte Carlo simulations. It can be used to compute the detection threshold for any given probability of false alarm. Compared with the MIMO-PGLRT detector, the MIMO-PSMI detector has a simpler structure and is computationally more efficient. Both detectors have the desirable CFAR property against the noise covariance matrix. Simulations results show that with a limited amount of secondary data, the two proposed detectors significantly outperform the conventional MIMO-GLRT and MIMO-AMF detectors, which do not exploit the persymmetric structure, and the MIMO-PGLRT detector performs better than the MIMO-PSMI detector. When the amount of secondary data is sufficient, all detectors considered in this paper achieve similar detection performance. Therefore, when the amount of secondary data is limited, the MIMO-PGLRT detector is recommended due to its superiority in detection performance, whereas when the amount of secondary data is sufficient, the MIMO-PSMI

detector is suggested because of its lower computation complexity.

APPENDIX A. A DERIVATION OF MIMO-PGLRT DETECTOR

Because the random variables $\mathbf{X}_{r,t}$ are independent, the maximization of the left-hand side of (5) can be performed term by term. Using (6), we can rewrite (5) as

$$\prod_{r=1}^{N}\prod_{t=1}^{M}\underbrace{\frac{\max_{\{a_{r,t},\mathbf{R}_{r,t}\}} f_{r,t,1}}{\max_{\{\mathbf{R}_{r,t}\}} f_{r,t,0}}}_{\triangleq\Upsilon_{r,t}}\underset{H_0}{\overset{H_1}{\gtrless}}\lambda_0. \tag{31}$$

In the following, we simplify $\Upsilon_{r,t}$ by using the approach in the case of a single band in [27]. Exploiting the persymmetric structure of $\mathbf{R}_{r,t}$, we have

$$\mathrm{tr}(\mathbf{R}_{r,t}^{-1}\mathbf{T}_{r,t,q}) = \mathrm{tr}(\mathbf{R}_{r,t}^{-1}\mathbf{J}\mathbf{T}_{r,t,q}^{*}\mathbf{J}). \tag{32}$$

Then,

$$\mathrm{tr}(\mathbf{R}_{r,t}^{-1}\mathbf{T}_{r,t,q}) = \mathrm{tr}(\mathbf{R}_{r,t}^{-1}\hat{\mathbf{T}}_{r,t,q}), \tag{33}$$

where

$$\hat{\mathbf{T}}_{r,t,q} = (\mathbf{T}_{r,t,q} + \mathbf{J}\mathbf{T}_{r,t,q}^{*}\mathbf{J})/2. \tag{34}$$

Using (8),$\hat{\mathbf{T}}_{r,t,q}$ can be rewritten as

$$\hat{\mathbf{T}}_{r,t,q} = \frac{\hat{\mathbf{R}}_{r,t} + (\widehat{\mathbf{X}}_{r,t} - q\ \mathbf{s}_{r,t}\hat{\mathbf{a}}_{r,t})(\widehat{\mathbf{X}}_{r,t} - q\ \mathbf{s}_{r,t}\hat{\mathbf{a}}_{r,t})^{\dagger}}{K_{r,t}+1}, \tag{35}$$

where

$$\hat{\mathbf{a}}_{r,t} = [\Re\mathfrak{e}(a_{r,t}),\ \jmath\Im\mathfrak{m}(a_{r,t})], \tag{36}$$

$$\hat{\mathbf{R}}_{r,t} = \frac{1}{2}\sum_{k=1}^{K_{r,t}}\{\mathbf{y}_{r,t}(k)\mathbf{y}_{r,t}^{\dagger}(k) + \mathbf{J}[\mathbf{y}_{r,t}(k)\mathbf{y}_{r,t}^{\dagger}(k)]^{*}\mathbf{J}\}, \tag{37}$$

and

$$\hat{\mathbf{X}}_{r,t} = [\hat{\mathbf{x}}_{r,t}^{\mathrm{e}}, \hat{\mathbf{x}}_{r,t}^{\mathrm{o}}] \tag{38}$$

with

$$\hat{\mathbf{x}}_{r,t}^{\mathrm{e}} = (\mathbf{x}_{r,t} + \mathbf{J}\mathbf{x}_{r,t}^{*})/2 \tag{39}$$

and

$$\hat{\mathbf{x}}_{r,t}^{\mathrm{o}} = (\mathbf{x}_{r,t} - \mathbf{J}\mathbf{x}_{r,t}^{*})/2. \tag{40}$$

According to [28], the ML estimates of $\mathbf{R}_{r,t}$ under H_0 and H_1 are $\hat{\mathbf{T}}_{r,t,0}$ and $\hat{\mathbf{T}}_{r,t,1}$, respectively. Using these ML estimates, we can write $\Upsilon_{r,t}$ defined in (31) as

$$\Upsilon_{r,t} = \left[\frac{\det(\hat{\mathbf{T}}_{r,t,0})}{\min_{\{\hat{\mathbf{a}}_{r,t}\}}\det(\hat{\mathbf{T}}_{r,t,1})}\right]^{K_{r,t}+1}. \tag{41}$$

It follows from (35) that

$$\det(\hat{\mathbf{T}}_{r,t,1}) = \frac{1}{(K_{r,t}+1)^{Q_t}}\det(\hat{\mathbf{R}}_{r,t})\det[\mathbf{I}_2 + (\hat{\mathbf{X}}_{r,t} - \mathbf{s}_{r,t}\hat{\mathbf{a}}_{r,t})^{\dagger}\hat{\mathbf{R}}_{r,t}^{-1}(\hat{\mathbf{X}}_{r,t} - \mathbf{s}_{r,t}\hat{\mathbf{a}}_{r,t})]. \tag{42}$$

It is straightforward that the value of $\hat{\mathbf{a}}_{r,t}$ minimizing the denominator of (41) is $(\mathbf{s}_{r,t}^{\dagger}\hat{\mathbf{R}}_{r,t}^{-1}\mathbf{s}_{r,t})^{-1}\mathbf{s}_{r,t}^{\dagger}\hat{\mathbf{R}}_{r,t}^{-1}\hat{\mathbf{X}}_{r,t}$. Substituting this ML estimate into (41) and after some algebraic manipulations, we can obtain

$$\Upsilon_{r,t} = \left(\frac{1}{1-\Phi_{r,t}}\right)^{K_{r,t}+1}, \tag{43}$$

where

$$\Phi_{r,t} = \frac{\tilde{\mathbf{s}}_{r,t}^{\dagger}\tilde{\mathbf{R}}_{r,t}^{-1}\tilde{\mathbf{X}}_{r,t}(\mathbf{I}_2 + \tilde{\mathbf{X}}_{r,t}^{\dagger}\tilde{\mathbf{R}}_{r,t}^{-1}\tilde{\mathbf{X}}_{r,t})^{-1}\tilde{\mathbf{X}}_{r,t}^{\dagger}\tilde{\mathbf{R}}_{r,t}^{-1}\tilde{\mathbf{s}}_{r,t}}{\tilde{\mathbf{s}}_{r,t}^{\dagger}\tilde{\mathbf{R}}_{r,t}^{-1}\tilde{\mathbf{s}}_{r,t}}. \tag{44}$$

Define two unitary matrices

$$\mathbf{D} = \frac{1}{2}[(\mathbf{I}+\mathbf{J}) + \jmath(\mathbf{I}-\mathbf{J})], \tag{45}$$

and

$$\mathbf{V} = \begin{bmatrix} 1 & 0 \\ 0 & -\jmath \end{bmatrix}. \tag{46}$$

Then, $\Phi_{r,t}$ in (44) can be rewritten in the real domain as

$$\Phi_{r,t} = \frac{\tilde{\mathbf{s}}_{r,t}^{\dagger}\tilde{\mathbf{R}}_{r,t}^{-1}\tilde{\mathbf{X}}_{r,t}(\mathbf{I}_2 + \tilde{\mathbf{X}}_{r,t}^{\dagger}\tilde{\mathbf{R}}_{r,t}^{-1}\tilde{\mathbf{X}}_{r,t})^{-1}\tilde{\mathbf{X}}_{r,t}^{\dagger}\tilde{\mathbf{R}}_{r,t}^{-1}\tilde{\mathbf{s}}_{r,t}}{\tilde{\mathbf{s}}_{r,t}^{\dagger}\tilde{\mathbf{R}}_{r,t}^{-1}\tilde{\mathbf{s}}_{r,t}}, \tag{47}$$

where

$$\tilde{\mathbf{X}}_{r,t} = \mathbf{D}\hat{\mathbf{X}}_{r,t}\mathbf{V}^{\dagger}, \tag{48}$$

$$\tilde{\mathbf{R}}_{r,t} = \mathbf{D}\hat{\mathbf{R}}_{r,t}\mathbf{D}^{\dagger} = \Re\mathfrak{e}(\hat{\mathbf{R}}_{r,t}) + \mathbf{J}\Im\mathfrak{m}(\hat{\mathbf{R}}_{r,t}), \tag{49}$$

and

$$\tilde{\mathbf{s}}_{r,t} = \mathbf{D}\mathbf{s}_{r,t} = \Re\mathfrak{e}(\mathbf{s}_{r,t}) - \Im\mathfrak{m}(\mathbf{s}_{r,t}). \tag{50}$$

Furthermore, $\tilde{\mathbf{X}}_{r,t}$ can be expressed as (12).

APPENDIX B. EQUIVALENT TRANSFORMATION OF Λ

First, we examine the possible range where the test statistic $\Phi_{r,t}$ can take values. As derived in [27, Eq. (B29)], the test statistic $\Phi_{r,t}$ can be transformed into

$$\Phi_{r,t} = 1 - [1 + \psi_{AA}\mathbf{W}(\mathbf{I}+\Sigma_B)^{-1}\mathbf{W}^{\dagger}]^{-1}, \tag{51}$$

where the quantity $\psi_{AA}\ \mathbf{W}(\mathbf{I} + \mathbf{\Sigma}_B)^{-1}\mathbf{W}^{\dagger}$ defined in [27] is a positive number. It is obvious that $0 < \Phi_{r,t} < 1$. Notice that the right-tail probability of the test statistic $\Phi_{r,t}$ is equal to its probability of false alarm. According to [27, Eq. (15)], the right-tail probability of $\Phi_{r,t}$ under hypothesis H_0 is

$$Pr(\Phi_{r,t} > \phi_{r,t}|H_0) = (1-\phi_{r,t})^{\frac{2K_{r,t}-Q_t+1}{2}}, \quad 0 < \phi_{r,t} < 1. \tag{52}$$

Then, the cumulative distribution function (CDF) of $\Phi_{r,t}$ under hypothesis H_0 is

$$Pr(\Phi_{r,t} < \phi_{r,t}|H_0) = 1 - (1-\phi_{r,t})^{\frac{2K_{r,t}-Q_t+1}{2}}. \tag{53}$$

Therefore, the PDF of $\Phi_{r,t}$ under hypothesis H_0 can be obtained by taking the derivative of the CDF with respect

to $\Phi_{r,t}$, namely,

$$f_{\Phi_{r,t}}(\phi_{r,t}) = \frac{2K_{r,t} - Q_t + 1}{2}(1 - \phi_{r,t})^{\frac{2K_{r,t}-Q_t-1}{2}}. \quad (54)$$

Define a monotone transform

$$\Omega_{r,t} = \frac{2K_{r,t} - Q_t + 1}{2} \ln \frac{1}{1 - \Phi_{r,t}}, \quad (55)$$

we can then obtain the PDF of $\Omega_{r,t}$ under hypothesis H_0

$$f_{\Omega_{r,t}}(\omega_{r,t}) = \exp(-\omega_{r,t}),\ \omega_{r,t} > 0. \quad (56)$$

Using (55), (17) can be written as

$$\Lambda = \sum_{r=1}^{N}\sum_{t=1}^{M} \alpha_{r,t}\Omega_{r,t} \underset{H_0}{\overset{H_1}{\gtrless}} \lambda, \quad (57)$$

where

$$\alpha_{r,t} = (2K_{r,t} + 2)/(2K_{r,t} - Q_t + 1). \quad (58)$$

For ease of notation, $\alpha_{1,1}, \ldots, \Phi_{1,M}, \ldots, \Phi_{N,1}, \ldots, \Phi_{N,M}$ are relabeled as $\alpha_1, \alpha_2, \ldots, \alpha_V$, respectively, where $V = MN$. Similarly, $\Omega_{1,1}, \ldots, \Omega_{N,M}$ are relabeled as Ω_1, $\Omega_2, \ldots, \Omega_V$, respectively. Then, (57) can be rewritten as

$$\Lambda = \sum_{i=1}^{V} \alpha_i \Omega_i \underset{H_0}{\overset{H_1}{\gtrless}} \lambda \quad (59)$$

where the random variable Ω_i under H_0 has the standard exponential distribution as in (56).

REFERENCES

[1] Li, J., and Stoica, P.
MIMO Radar Signal Processing.
Hoboken, NJ: John Wiley & Sons, 2009.

[2] He, Q., Blum, R. S., and Haimovich, A. M.
Noncoherent MIMO radar for location and velocity estimation: more antennas means better performance.
IEEE Transactions on Signal Processing, **58**, 7 (Jul. 2010), 3661–3680.

[3] He, Q., and Blum, R. S.
Diversity gain for MIMO Neyman-Pearson signal detection.
IEEE Transactions on Signal Processing, **59**, 3 (Mar. 2011), 869–881.

[4] Wang, S., He, Q., and He, Z.
LFM-based waveform design for cognitive MIMO radar with constrained bandwidth.
EURASIP Journal on Advances in Signal Processing, **89**, 1 (2014), 89–101.

[5] He, Q., and Blum, R. S.
Noncoherent versus coherent MIMO radar: performance and simplicity analysis.
Signal Processing, **92**, 10 (May 2012), 2454–2463.

[6] Li, J., and Stoica, P.
MIMO radar with colocated antennas.
IEEE Signal Processing Magazine, **24**, 5 (Sep. 2007), 106–114.

[7] Li, H., and Himed, B.
Transmit subaperturing for MIMO radars with co-located antennas.
IEEE Journal of Selected Topics in Signal Processing, **4**, 1 (Feb. 2010), 55–65.

[8] Cui, G., Li, H., and Rangaswamy, M.
MIMO radar waveform design with constant modulus and similarity constraints.
IEEE Transactions on Signal Processing, **62**, 2 (Jan. 2014), 343–353.

[9] Haimovich, A. M., Blum, R. S., and Cimini, L. J.
MIMO radar with widely separated antennas.
IEEE Signal Processing Magazine, **25**, 1 (Jan. 2008), 116–129.

[10] He, Q., Blum, R., Godrich, H., and Haimovich, A.
Target velocity estimation and antenna placement for MIMO radar with widely separated antennas.
IEEE Journal of Selected Topics in Signal Processing, **4**, 1 (Feb. 2010), 79–100.

[11] Zhou, S., Liu, H., Zhao, Y., and Hu, L.
Target spatial and frequency scattering diversity property for diversity MIMO radar.
Signal Processing, **91**, 2 (Feb. 2011), 269–276.

[12] Wang, P., Li, H., and Himed, B.
Moving target detection using distributed MIMO radar in clutter with nonhomogeneous power.
IEEE Transactions on Signal Processing, **59**, 10 (Oct. 2011), 4809–4820.

[13] De Maio, A., and Lops, M.
Design principles of MIMO radar detectors.
IEEE Transactions on Aerospace and Electronic Systems, **43**, 3 (Jul. 2007), 886–898.

[14] Wang, P., Li, H., and Himed, B.
A parametric moving target detector for distributed MIMO radar in non-homogeneous environment.
IEEE Transactions on Signal Processing, **61**, 9 (Apr. 2013), 1351–1356.

[15] Sheikhi, A., and Zamani, A.
Temporal coherent adaptive target detection for multi-input multi-output radars in clutter.
IET Radar, Sonar & Navigation, **2**, 2 (Apr. 2008), 86–96.

[16] Liu, J., Zhang, Z.-J., Cao, Y., and Yang, S.
A closed-form expression for false alarm rate of adaptive MIMO-GLRT detector with distributed MIMO radar.
Signal Processing, **93**, 9 (Sep. 2013), 2771–2776.

[17] He, Q., Lehmann, N. H., Blum, R. S., and Haimovich, A. M.
MIMO radar moving target detection in homogeneous clutter.
IEEE Transactions on Aerospace and Electronic Systems, **46**, 3 (Jul. 2010), 1290–1301.

[18] McDonald, K. F., and Blum, R. S.
Exact performance of STAP algorithms with mismatched steering and clutter statistics.
IEEE Transactions on Signal Processing, **48**, 10 (Oct. 2000), 2750–2763.

[19] Rangaswamy, M.
Statistical analysis of the nonhomogeneity detector for non-Gaussian interference backgrounds.
IEEE Transactions on Signal Processing, **53**, 6 (Jun. 2005), 2101–2111.

[20] Liu, J., Zhang, Z.-J., Yang, Y., and Liu, H.
A CFAR adaptive subspace detector for first-order or second-order Gaussian signals based on a single observation.
IEEE Transactions on Signal Processing, **59**, 11 (Nov. 2011), 5126–5140.

[21] De Maio, A.
Maximum likelihood estimation of structured persymmetric covariance matrices.
Signal Processing, **83**, 3 (Mar. 2003), 633–640.

[22] Conte, E., De Maio, A., and Farina, A.
Statistical tests for higher order analysis of radar clutter: their application to L-band measured data.
IEEE Transactions on Aerospace and Electronic Systems, **41**, 1 (Jan. 2005), 205–218.

[23] Aubry, A., De Maio, A., Pallotta, L., and Farina, A.
Maximum likelihood estimation of a structured covariance matrix with a condition number constraint.
IEEE Transactions on Signal Processing, **60**, 6 (Jun. 2012), 3004–3021.

[24] Aubry, A., De Maio, A., Pallotta, L., and Farina, A.
Radar detection of distributed targets in homogeneous interference whose inverse covariance structure is defined via unitary invariant functions.
IEEE Transactions on Signal Processing, **61**, 20 (Oct. 2013), 4949–4961.

[25] Zhou, S., Liu, H., Liu, B., and Yin, K.
Adaptive MIMO radar target parameter estimation with Kronecker-product structured interference covariance matrix.
Signal Processing, **92**, 5 (May 2012), 1177–1188.

[26] Van Trees, H. L.
Optimum Array Processing, Part IV of Detection, Estimation, and Modulation Theory. New York: Wiley-Interscience, 2002.

[27] Cai, L., and Wang, H.
A persymmetric multiband GLR algorithm.
IEEE Transactions on Aerospace and Electronic Systems, **28**, 3 (Jul. 1992), 806–816.

[28] Nitzberg, R.
Application of maximum likelihood estimation of persymmetric covariance matrices to adaptive processing.
IEEE Transactions on Aerospace and Electronic Systems, **AES-16**, 1 (Jan. 1980), 124–127.

[29] Cai, L., and Wang, H.
A persymmetric modified-SMI algorithm.
Signal Processing, **23**, 1 (Jan. 1991), 27–34.

[30] Conte, E., and De Maio, A.
Exploiting persymmetry for CFAR detection in compound-Gaussian clutter.
IEEE Transactions on Aerospace and Electronic Systems, **39**, 2 (Apr. 2003), 719–724.

[31] Casillo, M., De Maio, A., Iommelli, S., and Landi, L.
A persymmetric GLRT for adaptive detection in partially-homogeneous environment.
IEEE Signal Processing Letters, **14**, 12 (Dec. 2007), 1016–1019.

[32] Pailloux, G., Forster, P., Ovarlez, J.-P., and Pascal, F.
Persymmetric adaptive radar detectors.
IEEE Transactions on Aerospace and Electronic Systems, **47**, 4 (Oct. 2011), 2376–2390.

[33] Hao, C., Orlando, D., Ma, X., and Hou, C.
Persymmetric Rao and Wald tests for partially homogeneous environment.
IEEE Signal Processing Letters, **19**, 9 (Sep. 2012), 587–590.

[34] Wang, P., Sahinoglu, Z., Pun, M.-O., and Li, H.
Persymmetric parametric adaptive matched filter for multichannel adaptive signal detection.
IEEE Transactions on Signal Processing, **60**, 6 (Jun. 2012), 3322–3328.

[35] Gao, Y., Liao, G., Zhu, S., and Yang, D.
A persymmetric GLRT for adaptive detection in compound-Gaussian clutter with random texture.
IEEE Signal Processing Letters, **21**, 6 (Jun. 2013), 615–618.

[36] Hao, C., Orlando, D., Foglia, G., Ma, X., Yan, S., and Hou, C.
Persymmetric adaptive detection of distributed targets in partially-homogeneous environment.
Digital Signal Processing, **24**, (Jan. 2014), 42–51.

[37] Ali, M. M., and Obaidullah, M.
Distribution of linear combination of exponential variates.
Communications in Statistics-Theory and Methods, **11**, 13 (1982), 1453–1463.

[38] Liu, J., Zhang, Z.-J., Shui, P.-L., and Liu, H.
Exact performance analysis of an adaptive subspace detector.
IEEE Transactions on Signal Processing, **60**, 9 (Sep. 2012), 4945–4950.

Jun Liu (S'11–M'13) received the B.S. degree in mathematics from Wuhan University of Technology, China, in 2006, the M.S. degree in mathematics from Chinese Academy of Sciences, China, in 2009, and the Ph.D. degree in electrical engineering from Xidian University, China, in 2012. From July 2012 to December 2012, he was a postdoctoral research associate in the Department of Electrical and Computer Engineering, Duke University, Durham, NC. From January 2013 to September 2014, he was a Post-doctoral Research Associate in the Department of Electrical and Computer Engineering, Stevens Institute of Technology, Hoboken, NJ, USA. He is now with the National Laboratory of Radar Signal Processing, Xidian University, where he is an Associate Professor.

His research interests include statistical signal processing, optimization algorithms, passive sensing, and MIMO radar.

Hongbin Li (M'99–SM'08) received the B.S. and M.S. degrees from the University of Electronic Science and Technology of China in 1991 and 1994, respectively, and the Ph.D. degree from the University of Florida, Gainesville, FL, in 1999, all in electrical engineering.

From July 1996 to May 1999, he was a research assistant in the Department of Electrical and Computer Engineering at the University of Florida. Since July 1999, he has been with the Department of Electrical and Computer Engineering, Stevens Institute of Technology, where he is a professor. He was a summer visiting faculty member at the Air Force Research Laboratory in the summers of 2003, 2004, and 2009. His general research interests include statistical signal processing, wireless communications, and radars.

Dr. Li received the IEEE Jack Neubauer Memorial Award in 2013 for the best systems paper published in the *IEEE Transactions on Vehicular Technology*, the Outstanding Paper Award from the IEEE AFICON Conference in 2011, the Harvey N. Davis Teaching Award in 2003, the Jess H. Davis Memorial Award for excellence in research in 2001 from Stevens Institute of Technology, and the Sigma Xi Graduate Research Award from the University of Florida in 1999. He has been a member of the IEEE SPS Signal Processing Theory and Methods (2011 to now) Technical Committee (TC) and the IEEE SPS Sensor Array and Multichannel TC (2006–2012). He is an Associate Editor for *Signal Processing* and served on the editorial boards for *IEEE Transactions on Wireless Communications*, *IEEE Signal Processing Letters*, and *IEEE Transactions on Signal Processing*. He was a Guest Editor for *EURASIP Journal on Applied Signal Processing*. He has been involved in various conference organization activities, including serving as a General Co-Chair for the 7th IEEE Sensor Array and Multichannel Signal Processing (SAM) Workshop, Hoboken, NJ, June 17–20, 2012. Dr. Li is a member of Tau Beta Pi and Phi Kappa Phi.

Braham Himed (S'88–M'90–SM'01–F'07) received his B.S. degree in electrical engineering from Ecole Nationale Polytechnique of Algiers in 1984, and his M.S. and Ph.D. degrees, both in electrical engineering, from Syracuse University in 1987 and 1990, respectively. Dr. Himed is a technical advisor with the Air Force Research Laboratory, Sensors Directorate, RF Technology Branch, where he is involved with several aspects of radar developments. His research interests include detection, estimation, multichannel adaptive signal processing, time series analyses, array processing, space-time adaptive processing, waveform diversity, MIMO radar, passive radar, and over the horizon radar. Dr. Himed is the recipient of the 2001 IEEE region I award for his work on bistatic radar systems, algorithm development, and phenomenology. Dr. Himed is a Fellow of the IEEE and a member of the AES Radar Systems Panel. Dr. Himed is the recipient of the 2012 IEEE Warren White award for excellence in radar engineering. Dr. Himed is also a Fellow of AFRL (Class of 2013).